

GT2003-38356

A NEW PARADIGM FOR SIMULATION OF TURBULENT COMBUSTION IN REALISTIC GAS TURBINE COMBUSTORS USING LES

G. Constantinescu

Center for Integrated Turbulence Simulations
Department of Mechanical Engineering
Bldg. 500, Stanford University,
Stanford, California 94305-3030
Email: gconstan@ctr.stanford.edu

K. Mahesh

Department of Aerospace
Engineering and Mechanics
University of Minnesota
Minneapolis, MN 55455
Email: mahesh@aem.umn.edu

S. Apte

Center for Integrated Turbulence Simulations
Department of Mechanical Engineering
Bldg. 500, Stanford University,
Stanford, California 94305-3030
Email: sapte@stanford.edu

G. Iaccarino

Center for Turbulence Research
Stanford University
Stanford, California, 94305
Email: jops@ctr.stanford.edu

F. Ham

Center for Turbulence Research
Stanford University
Stanford, California, 94305
Email: fham@stanford.edu

P. Moin

Center for Turbulence Research
Stanford University
Stanford, California, 94305
Email: moin@ctr.stanford.edu

ABSTRACT

This paper presents a new paradigm for numerical simulation of turbulent combustion in realistic gas turbine combustors. Advanced CFD methods using Large Eddy Simulation (LES) turbulence models are central to this paradigm in fluid dynamics where engineers can apply the full predictive abilities of numerical simulations to the design of realistic gas turbine combustors. The use of LES models is motivated by their demonstrated superiority over RANS to predict turbulent mixing. The subgrid scale models incorporated in LES are based on the dynamic approach where the model coefficients are computed rather than prescribed by the user. This has provided unparalleled robustness to modern turbulent flow computations using LES. A new numerical algorithm was derived that is discretely energy conserving on hybrid unstructured grids, thus allowing numerical simulations at high Reynolds numbers corresponding to operating conditions without using artificial numerical dissipation. This paper deals specifically with the simulation of the gas phase flow through realistic gas turbine combustors and the implementation of combustion and spray models that are needed to predict and control the combustion phenomena in these geometries. Results from several simulations and comparison with experimental data are used to validate this approach. In particular, a complete simulation of the unsteady flow field in a realistic combustor geometry is carried out. Some preliminary results

for reacting flow simulations in gas turbine combustors are also discussed. We discuss several challenges related to large-scale simulations of the flow in realistic combustors, including methods to further accelerate the algorithm's convergence (e.g., use of multigrid techniques), improvement of the parallel performance of the flow solver for two-phase flow simulations (e.g., use of dynamic load balancing that accounts for the additional CPU time spent in the spray module when particles are present in the cells).

INTRODUCTION

Computational Fluid Dynamics (CFD) plays an important role in the design of gas turbine engines. Steady-state calculations using RANS models are commonly used in the design of the individual components of the engines, including the combustor. However, due to the very complex geometry and flow that develops in the combustor, the predictive capabilities of RANS models are rather limited. Capturing the dynamically important coherent eddies in such complex flows, in which accurate simulation of turbulent mixing phenomena related to turbulent combustion is essential, requires turbulent models and numerical methods that have this capability. In the work reported in this paper, the

large eddy simulation (LES) approach is used to simulate the flow through the combustor of a gas turbine engine. The main reason for the lack of LES simulations of these flows are the large computational requirements necessary to calculate the flow solutions and the long integration times necessary to converge the statistics. However, the development of massively parallel computer systems starts making possible the use of LES for predicting flows of industrial interest. The combustor simulations have two major components - gas phase and sprays. Simulation of the gas phase flow is performed using a newly developed parallel, unstructured grid LES solver which has been completely integrated with the spray module. The gas phase solver (see Mahesh et al., 2001, 2002 for more details) is non-dissipative and discretely conserves energy, thus insuring both accuracy and robustness for high Reynolds number simulations in complex geometries. A dynamic procedure is used to compute the coefficients in the additional terms that are present in the filtered momentum and scalar-transport equations.

The main objective of this work is to develop unstructured mesh technology for LES of reacting flow (including spray physics) in realistic configurations using massively parallel computing platforms. One of the main goals in the development of the present LES code was to ensure that the solver scales well up to a high number of processors (in the range of several hundreds to couple of thousands) so that problems of far larger size than the usual size used in design calculations can be simulated efficiently. The code was parallelized using the Message Passing Interface (MPI) and was shown to scale well (up to 1,000 processors in some cases) on several of today's most advanced parallel computers, including the INTEL-ASCI RED machine at the Sandia National Laboratory, the latest IBM SP3 at the Lawrence Livermore National Laboratory and the Origin2000 system at Stanford University. Intensive validation has been an intrinsic part of the development of the present LES solver and results for flows in complex combustor geometries are reported in this paper. These test cases include non-reacting flow in a full Pratt & Whitney geometry and in a front-end Pratt & Whitney combustor geometry, an atomization experiment in the same front-end geometry and preliminary results for a reacting flow simulation in the full combustor geometry. Our final objective is to use this code for prediction, analysis and design of gas turbine combustors.

NUMERICAL METHOD

Implicit versus Explicit solver

The original gas-phase solver we developed used the explicit second-order Adams-Bashforth method coupled with

a fractional-step method to advance the Navier-Stokes equations in time. Algorithmic developments in the gas-phase solver emphasized spatial discretization which resulted in the development of a non-dissipative, energy-conserving formulation in the absence of time-discretization errors (for more details see Mahesh et al., 2003a and 2003b). This explicit algorithm was successfully used to demonstrate the accuracy of the flow solver in both simple and exceedingly complex geometries such as a Pratt & Whitney combustor. A detailed description of the validation simulations using the explicit incompressible flow solver is given in Mahesh et al. (2001). These validation simulations showed that the accuracy obtained with the present LES code is comparable to the one obtained using established second-order accurate structured LES codes provided that the level of grid refinement and the LES sub-grid models used in these simulations are similar.

The main problem in using the explicit solver for predicting the flow in combustors of realistic geometry was the limitations in terms of the maximum physical time step that can be used in these calculations while maintaining convergence. These limitations in the time step were due to the numerical stability restrictions imposed by the Adams-Bashforth method. For instance, in a simulation of the swirling flow in a coaxial combustor geometry (see Mahesh et al., 2001 and Sommerfeld & Qiu, 1991) we found that the maximum time step in the present LES code had to be chosen about an order of magnitude less than the time-step used by Pierce & Moin (2001) in their structured grid computations that treated the viscous terms implicitly. Also the simulations performed in the front-end model (to be discussed later) showed that the narrow passages in the fuel injector considerably accelerate the flow, and thereby the convective terms impose strict restrictions on the time-step for an explicit scheme.

Recently (Mahesh et al, 2003b), to address the time-step restrictions, we implemented a fully implicit version of the gas-phase solver. In the implicit version, the second-order Crank-Nicholson scheme is used for both convection and viscous terms in the momentum equations. The convection terms are linearized prior to solution. The implementation is such that only the viscous terms can be implicitly advanced, if so desired. Presently successive-over relaxation is used to solve the implicit system. Typically 20 - 100 iterations are needed to converge the residuals. The use of multigrid techniques to solve the implicit system is under consideration (see next section for more details). Results for some typical calculations are summarized in Table 1. The savings are seen to be significant. For example, explicit calculation of the cold flow in a coaxial combustor geometry required 320 hours \times 96 processors = 30,700 CPU hours on an IBM SP3 machine. The implicit code uses

	Grid	Proc.	Explicit	Implicit
	10^6 cv's		CPU h	CPU h
Coaxial combustor	1.6	96	30700	5000
Channel $Re_\tau = 180$	0.9	32	2240	256
P & W combustor	1.4	32	13500	3200

Table 1. CPU TIME IN HOURS FOR THE EXPLICIT AND IMPLICIT SOLVER.

around 5,000 CPU hours, which is approximately a factor of 4 times the time taken by the highly optimized structured grid solver of Pierce and Moin that uses the same time-step. The cold flow calculations in complex geometries show significant speed-up due to the implicit algorithm. The above ratio of implicit to explicit time-step (6 to 7) also applies to the reacting flow simulations, to be discussed later.

Convergence acceleration using Multigrid techniques

In the present unstructured LES solver, the conjugate-gradient (cg) solution of the pressure-Poisson system is the most computationally expensive component of the overall solution process, requiring from 50 to 80% of the total solution time. This section presents some details of a multigrid solver for this Poisson system that will eventually replace the present cg solver. Tests using a single coarse grid (1-level multigrid) have demonstrated an overall reduction in computation time of 35 to 60% per time step. Once fully implemented, the pressure solver should become one of the least expensive components of the solution process, yielding reductions in overall computation time of 45 to 75% per time step.

The multigrid method currently being integrated into the unstructured LES solver has the following characteristics:

- V-cycle multigrid with linear restriction and block correction.
- Gauss-Seidel smoothing on all grids but the coarsest; on the coarsest grid, the residual is reduced by 1 order of magnitude using a coarse grid version of the present cg solver.
- Coarse grid control volumes are built by the agglomeration of fine grid control volumes. The agglomeration procedure is performed once per computation, when the pressure solver is first called. Agglomeration avoids use

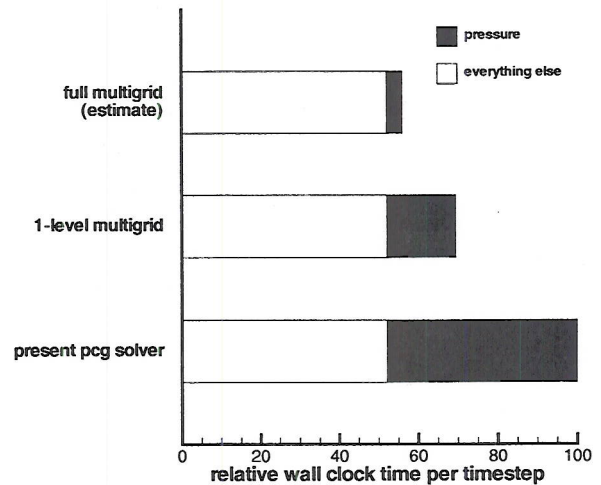


Figure 1. COMPARISON OF WALL CLOCK TIME PER TIME STEP FOR 3 DIFFERENT PRESSURE POISSON SOLVERS; COAXIAL COMBUSTOR PROBLEM WITH 1.1 MILION CONTROL VOLUMES, 32 PROCESSORS.

of mesh generators to generate the coarse grids, and simplifies the restriction and prolongation operators.

- Directional agglomeration (semi-coarsening) is used to prevent stalling of the multigrid method in the presence of large cell aspect ratios and the resulting coefficient anisotropy.
- Coarse grid coefficients are calculated using the discretized coarse grid approximation (i.e., geometric multigrid). Algebraic multigrid with 1st-order restriction (insertion) of the fine grid coefficients was tested and found to yield significantly slower convergence rates.

A two-grid version of this multigrid method has been added to the parallel unstructured LES solver and tested on a number of problems, including the coaxial combustor (1.1 million control volumes, 32 processors). Figure 1 compares the normalized wall-clock time per time step for this problem, breaking out the pressure solver from the other components of the solution (scalar equations, momentum equations, chemistry, etc.). For the coaxial combustor problem, the pressure solution requires about 50% of the total solution time when the present cg solver is used.

1-level multigrid is able to converge the pressure equation to the same tolerance in about 10 to 12 cycles, however each cycle is significantly more expensive than a fine grid cg iteration, so the actual speedup in pressure solution is

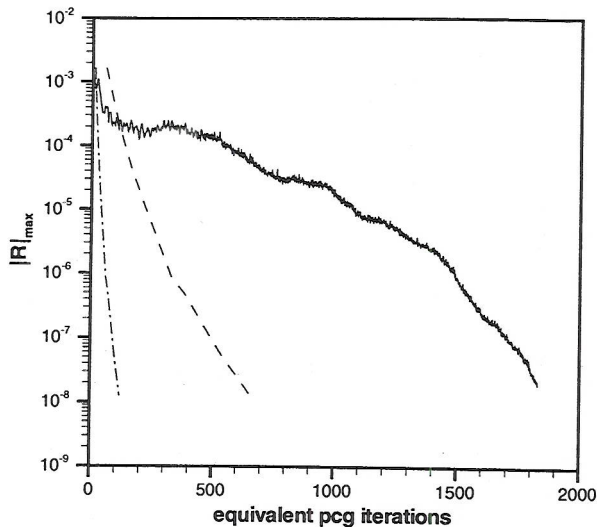


Figure 2. COMPARISON OF PRESSURE CONVERGENCE HISTORY DURING A TYPICAL TIME STEP FOR COAXIAL COMBUSTOR: — PRESENT CG SOLVER; - - - 1-LEVEL MULTIGRID; - · - · FULL MULTIGRID (ESTIMATE).

about 2.7 times, corresponding to a reduction in overall solution time of about 30%. Extrapolating this demonstrated two-grid performance to multiple coarse grids, the speedup in the pressure solution should be about 10 times, corresponding to a reduction in overall solution time of about 45% for this problem.

Figure 2 compares the convergence history of the the pressure solver for these three cases. The histories are plotted relative to "equivalent cg iterations", proportional to wall clock time.

COMBUSTION MODEL AND ITS IMPLEMENTATION IN THE UNSTRUCTURED SOLVER

In this section we present the motivation behind using the flamelet / progress variable combustion model developed by Pierce and Moin (2001) along with an overview of their method including the equations and the algorithm to calculate the subgrid momentum and scalar transport terms and its implementation in the unstructured code. Pierce and Moin's approach is based on "quasi-steady" flamelets in which the local flame state undergoes unsteady evolution through a sequence of stationary solutions to the flamelet equations.

A single-parameter flamelet library is first developed for

the given combustor conditions by looking for stationary solutions to the one-dimensional reaction-diffusion equations. The unstable and the lower branches of the S-shaped curve are included so that the complete range of flame states, from completely extinguished (mixing without reaction) to completely reacted (equilibrium chemistry), is represented in the library. Arbitrarily complex chemical kinetic mechanisms as well as differential-diffusion effects can be included. The result is a complete set of flame states, given in terms of mixture fraction and a single flamelet parameter (typically the dissipation rate), denoted by λ :

$$\begin{aligned} y_k &= y_k(Z, \lambda), & T &= T(Z, \lambda), \\ \rho &= \rho(Z, \lambda), & w_k &= w_k(Z, \lambda) \end{aligned} \quad (1)$$

where y_k are the mass fractions of the chemical species, T is the temperature, ρ the density, w_k are the reaction terms in the scalar transport equation for the chemical species and Z is the mixture fraction. One of the combustion variables, or some combination of the variables that is representative of the overall flame behavior is chosen to serve as an overall reaction progress variable.

In this model in addition to the variable density momentum and continuity equations (equations 2 and 3), scalar transport equations are solved for the mixture fraction Z , which is a conserved scalar (equation 4), and for the progress variable C , which is a non-conserved scalar (equation 5).

$$\frac{\partial \rho \mathbf{u}}{\partial t} + \nabla \cdot (\rho \mathbf{u} \mathbf{u}) = -\nabla p + \nabla \cdot [2\mu(\mathbf{S} - \frac{1}{3}\mathbf{I} \nabla \cdot \mathbf{u})] \quad (2)$$

$$\nabla \cdot (\rho \mathbf{u}) = -\frac{\partial \rho}{\partial t} \quad (3)$$

$$\frac{\partial \rho Z}{\partial t} + \nabla \cdot (\rho \mathbf{u} Z) = \nabla \cdot (\rho \alpha \nabla Z) \quad (4)$$

$$\frac{\partial \rho C}{\partial t} + \nabla \cdot (\rho \mathbf{u} C) = \nabla \cdot (\rho \alpha \nabla C) + \rho w_C \quad (5)$$

In the above equations, \mathbf{S} is the strain-rate tensor, \mathbf{I} is the identity tensor, μ is the molecular viscosity, α is the molecular diffusivity and w_C is the chemical reaction source term.

The continuity equation acts as a constraint on the velocity field, with the time-derivative of density as a source term. This constraint is enforced by the pressure, in a manner analogous to the enforcement of the incompressibility constraint for constant density flows.

Under the model assumptions, all the other fluid and flow variables (density, temperature, molecular viscosity, molecular diffusivity), chemical species and the reaction source terms in the scalar transport equations are related to the mixture fraction and the progress variable through a flamelet library that is precalculated given a specific fuel reaction mechanism and the flow conditions in the combustor. The only requirement for the quantity chosen to serve as progress variable is to be a quantity that is representative of the overall gross flame behavior and that varies monotonically with the flame state so that its value uniquely determines it.

The flamelet / progress variable approach can also be interpreted as a type of 'unsteady' flamelet model in the sense that the equivalent flamelet equation contains an unsteady term. However, instead of explicitly solving the unsteady flamelet equations, the unsteady evolution is actually embedded in the progress-variable transport equation, where the reaction and dissipation rates directly affect the evolution of the progress variable in a manner similar to the classical unsteady flamelet equations (Peters, 1984).

For turbulent simulations, the governing equations (2) to (5) are filtered. A major modeling requirement is for the nonlinear density function $\bar{\rho}$ obtained by filtering the state relation for the density ρ in (1). While algebraic scaling laws and scale-similarity concepts can be expected to work for quadratic nonlinearities, the only acceptable closure for arbitrary nonlinearities appears to be the probability density function (PDF) approach. Here, the presumed subgrid pdf is used:

$$\bar{\rho}^{-1} = \int \rho^{-1}(Z, \lambda) \tilde{P}(Z, \lambda) dZ d\lambda \quad (6)$$

In addition, the filtered progress variable equation contains a reaction source term \tilde{w}_C that must be closed. This is accomplished by writing

$$\tilde{w}_C = \int w_C(Z, \lambda) \tilde{P}(Z, \lambda) dZ d\lambda \quad (7)$$

and assuming that

$$\tilde{P}(Z, \lambda) = \tilde{P}(\lambda, \tilde{\lambda}) \cdot \beta(Z, \tilde{Z}, \tilde{Z}''^2) \quad (8)$$

where

$$\tilde{P}(\lambda, \tilde{\lambda}) = \frac{1}{\lambda\sqrt{2\pi}} \exp\left[-\frac{(\ln(\lambda) - \tilde{\lambda})^2}{2}\right] \quad (9)$$

That is, each subgrid state is represented by a single flamelet. For conserved scalars such as mixture fraction, the subgrid pdf is modeled using the beta distribution which is a reasonable assumption in the absence of further information about the subgrid state (Wall *et al.*, 2000). The log-normal distribution $\tilde{P}(\lambda, \tilde{\lambda})$ has been found in numerical experiments to provide an accurate description of gradient magnitude and dissipation rate fluctuations of conserved scalars in fully developed turbulence and is used in the present work. The final step is to relate the filtered dissipation rate parameter $\tilde{\lambda}$ to the filtered value of the progress variable, \tilde{C} that is obtained by solving the corresponding transport equation:

$$\tilde{C} = \int C(Z, \lambda) \tilde{P}(Z, \lambda) dZ d\lambda \quad (10)$$

After substitution of the presumed pdf and integrating, this yields

$$\tilde{C} = f(\tilde{Z}, \tilde{Z}''^2, \tilde{\lambda}) \quad (11)$$

If \tilde{C} is a monotonic function of $\tilde{\lambda}$, then the above relation can be used to eliminate $\tilde{\lambda}$ from the problem. The final result is a closed specification of the chemical system and fuel properties (molecular viscosity and molecular diffusivity) in terms of three variables \tilde{Z} , \tilde{Z}''^2 and \tilde{C} , which are chosen as the input variables in the chemical table for turbulent calculations:

$$y_k = y_k(\tilde{Z}, \tilde{Z}''^2, \tilde{C}), T = T(\tilde{Z}, \tilde{Z}''^2, \tilde{C}),$$

$$\rho = \rho(\tilde{Z}, \tilde{Z}''^2, \tilde{C}), w_k = w_k(\tilde{Z}, \tilde{Z}''^2, \tilde{C}) \quad (12)$$

$$\mu = \mu(\tilde{Z}, \tilde{Z}''^2, \tilde{C}), \alpha = \alpha(\tilde{Z}, \tilde{Z}''^2, \tilde{C}) \quad (13)$$

The subgrid mixture fraction variance \tilde{Z}''^2 is obtained using the method proposed by Pierce and Moin:

$$\rho \tilde{Z}''^2 = C_Z \bar{\rho} \Delta^2 |\nabla \tilde{Z}|^2 \quad (14)$$

where the coefficient C_Z is calculated dynamically. The subgrid momentum and scalar transport terms that appear

from the filtering of equations (2), (4) and (5) have to be modeled. The eddy viscosity μ_t and eddy diffusivity α_t that appear in these terms are evaluated as follows:

$$\mu_t = C_\mu \bar{\rho} \Delta^2 |\tilde{S}|, \quad \rho \alpha_t = C_\alpha \bar{\rho} \Delta^2 |\tilde{S}| \quad (15)$$

where the coefficients C_μ and C_α are calculated dynamically.

All the operators in the scalar transport equations are discretized in a similar fashion to the one used in the momentum equations.

SPRAY MODELS IMPLEMENTED IN LES CODE

Next, we provide a short overview of the Lagrangian particle-tracking scheme used in two-phase flow simulations and its integration with the unstructured gas-phase solver. The droplets are modeled as point particles which satisfy Lagrangian equations. They influence the gas phase through source terms in the gas-phase equations. As the particles move, their position is located and each particle is assigned to a control volume of the gas-phase grid. The gas-phase properties are interpolated to the particle location and the particle equations are advanced. The particles are then relocated, particles that cross interprocessor boundaries are duly transferred, source terms in the gas-phase equation are computed, and the computation is further advanced. More details on the Lagrangian particle-tracking module including validation (e.g., particle laden swirling flow in a co-axial combustor geometry corresponding to the experiment of Sommerfeld & Qiu, 1991) are provided in Mahesh et al. (2001, 2002). The incorporation of complex spray breakup models and of a hybrid particle-parcel technique needed for simulations with very large number of droplets (e.g., spray atomization in combustion) are described below. Evaporation is handled using a standard d^2 law model.

Stochastic model for secondary breakup

Liquid spray atomization plays a crucial role in the combustion dynamics in gas-turbine combustors. In standard Lagrangian particle tracking codes, emphasis is placed on obtaining the correct spray evolution characteristics away from the injector. Only the global behavior of the primary atomization, occurring close to the injector, is considered and the details are not captured. The essential features of spray evolution, viz. droplet size distribution, spray angle, and penetration depth, are predicted away from the injector surface by secondary breakup models. Usually standard, deterministic breakup models based on Taylor Analogy Breakup (TAB) (O'Rourke & Amsden 1987) or wave

(Reitz 1987) models are employed in RANS-type computations. Liquid 'blobs' with the size of the injector diameter are introduced into the combustion chamber and undergo atomization according to the balance between aerodynamic and surface tension forces acting on the liquid phase. Both models are deterministic with 'single-scale' production of new droplets. In many combustion applications, however, injection of liquid jet takes place at high relative velocity between the two phases (high initial Weber number). Under these conditions, intriguing processes such as turbulence-induced breakup, multiple droplet collision in the dense spray region, fluctuations due to cavitating flow inside the injector, etc., contribute to the process of atomization. This results in droplet formation over a large spectrum of droplet-sizes and is not captured by the above models. Predicting the distribution of droplet sizes at each spray location is important for sheet-breakup modeling.

In order to predict the essential global features of these complex phenomena, a stochastic approach for droplet breakup which accounts for a range of product-droplet sizes is necessary. Specifically, for a given control volume, the characteristic radius of droplets is assumed to be a time-dependent stochastic variable with a given initial distribution function. The breakup of parent blobs into secondary droplets is viewed as the temporal and spatial evolution of this distribution function around the parent-droplet size. This distribution function follows a certain long-time behavior, which is characterized by the dominant mechanism of breakup. The size of new droplets is then sampled from the distribution function evaluated at a typical breakup time scale of the parent drop.

Owing to the complexity of the phenomenon, it is difficult to clearly identify such a dominant mechanism for breakup. Kolmogorov (1941) developed a stochastic theory for breakup of solid particles by modeling it as a discrete random process. He assumed that the probability to break each parent particle into a certain number of parts is independent of the parent-particle size. Using central limit theorem, Kolmogorov pointed out that such a general assumption leads to a log-normal distribution of particle size in the long-time limit.

Based on Kolmogorov's hypothesis we have developed a numerical scheme for atomization of liquid spray at large Weber number (Gorokhovski & Apte, 2001). The discrete model by Kolmogorov is reformulated in terms of a Fokker-Planck (FP) differential equation for the evolution of the size-distribution function from a parent-blob towards the log-normal law:

$$\frac{\partial T(x, t)}{\partial t} + \nu(\xi) \frac{\partial T(x, t)}{\partial x} = \frac{1}{2} \nu(\xi^2) \frac{\partial^2 T(x, t)}{\partial x^2} \quad (16)$$

where the breakup frequency (ν) and time (t) are introduced. Here, $T(x, t)$ is the distribution function for $x = \log(r_j)$, where r_j is the droplet radius. Breakup occurs when $t > t_{breakup} = 1/\nu$. The value of the breakup frequency and the critical radius of breakup are obtained by the balance between the aerodynamic and surface tension forces. The secondary droplets are sampled from the analytical solution of equation (16) corresponding to the breakup time-scale. The parameters encountered in the FP equation ($\langle \xi \rangle$ and $\langle \xi^2 \rangle$) are computed by relating them to the local Weber and Reynolds numbers for the parent blob, thereby accounting for the capillary forces and turbulent properties. The capillary force prescribes a lower bound limit for the produced-droplet size through the local maximum stable (or critical) radius (r_{cr}). The velocity of the produced droplets is modeled using Monte-Carlo procedure. As new droplets are formed, parent droplets are destroyed and Lagrangian tracking in the physical space is continued till further breakup events. The evolution of droplet diameter is basically governed by the local relative-velocity fluctuations between the gas and liquid phases. In this respect, LES plays a key role in providing accurate, local estimates of the gas-phase turbulent quantities. Although the mesh spacing used in a typical LES computation is larger than droplet size, the superiority of LES over RANS lies in accurate predictions of mixing and momentum transport from the gas phase to the spray field. The details of this model are given in Gorokhovski & Apte (2001).

Hybrid particle-parcel technique for spray simulations

Performing spray breakup computations using Lagrangian tracking of each individual droplet gives rise to a large number of droplets (50-100 millions) very close to the injector. Computing such a large number of droplet trajectories is a formidable task even with supercomputers. In parallel computation of complex flows utilizing standard domain-decomposition techniques, the load balancing per processor is achieved by equally distributing the number of grid cells among all processors. Lagrangian particle-tracking, however, causes load-imbalance owing to the varying number of droplets per processor.

In order to overcome the above load balancing problem, the usual approach is to represent a group of droplets with similar characteristics (diameter, velocity, temperature etc..) by a computational particle or 'parcel'. In addition, one carries the number of droplets per parcel as a parameter to be tracked. Since, a parcel represents a group of droplets (of the order of 100-1000), the total number of computational particles or trajectories to be simulated is reduced significantly. With breakup, the diameter of the parcel is sampled according to the procedure given above and the

number of droplets associated with the particles is changed in order to conserve mass. This reduces the total number of particles per processor and increases the computational overhead with sprays by around 20% depending on the number of parcels used. Each parcel has all the droplet characteristics associated with it. The parcels-methodology works well for RANS-type simulations where one is interested in time- or ensemble-averaged quantities. For LES, however, we should ideally simulate as many droplet trajectories as possible in order to obtain time-accurate results.

A hybrid scheme involving the computation of both individual droplets and parcels is proposed. The difference between droplets and parcels is simply the number of particles associated with them, N_{par} , which is unity for droplets. During injection, new particles added to the computational domain are pure drops ($N_{par} = 1$). These drops move downstream and undergo breakup according to the above breakup model and produce new droplets. This increases the number of computational particles in the domain. In the dense-spray regime, one may obtain large number of droplets in a control volume and its immediate neighbors. The basic idea behind the hybrid-approach, is to collect all droplets in a particular control volume and group them into bins corresponding to their size and other properties such as velocity, temperature etc. The droplets in bins are then used to form a parcel by conserving mass, momentum and energy. The properties of the parcel are obtained by mass-weighted averaging from individual droplets in the bin. For this procedure, only those control volumes are considered for which the number of droplets increases above a certain threshold value. The number of parcels created would depend on the number of bins and the threshold value used to sample them. The parcel thus created then undergoes breakup according to the above stochastic sub-grid model, however, does not create new parcels. On the other hand, N_{par} is increased and the diameter is decreased by mass-conservation.

COLD FLOW SIMULATIONS IN THE PRATT & WHITNEY GEOMETRY

The reader is referred to Mahesh et al. (2001, 2002, 2003a and 2003b) for a detailed discussion of the validation simulations of the present solver for a wide range of laminar and turbulent flows including isotropic turbulence, channel flows, flow over cylinders, flow in co-axial combustors, etc. The same references also contain results from numerical simulations that were used to validate the different components of the reacting-flow solver including the Lagrangian particle-tracking procedure, the atomization and evaporation models. These tests included the particle-laden flow in a co-axial combustor, atomization in a Diesel engine

combustion chamber, evaporation in a co-axial combustor, etc. In this section we focus on the simulations performed in complex realistic gas turbine combustor geometries. RANS simulations of the flow in combustors of geometric complexity comparable to the present ones were reported recently by Crocker et al. (1998), Eccles and Priddin (1999), Birkby et al. (2000) and Malecki et al. (2001). The most complex RANS models used in these simulations were linear two-equation eddy-viscosity models. We are not aware of any LES attempt to simulate the flow in full combustor geometries that include the injectors, inner and outer diffuser passages, dilution holes, etc.

A general question that arises is whether or not the additional computational resources needed to perform LES in such geometries is justified. As the final purpose of the present work is to perform a fully integrated simulation of an entire jet engine including the turbines and compressors (for which an unsteady RANS code is being used) we are interested in time accurate calculations of the flow in the combustor (for instance, the flow coming from the compressor is always unsteady due to the finite number of blades). Thus, a fair comparison will be between a time-accurate RANS simulation and an LES simulation of the same flow. In this case the computational resources needed to perform the two computations are rather comparable, though still larger in LES due to the fact that one should have a sufficient fine mesh to accurately capture the dynamically important eddies in the main combustion chamber. The reason for which LES is not too expensive for this kind of flows is that in the main combustion chamber where combustion takes place the flow is not determined by the wall attached boundary layers. The main dynamics in the combustion chamber is determined by the jets coming out of the injectors and dilution holes. So, one does not need to accurately resolve the attached boundary layers inside the injector channels or close to the lateral walls of the combustion chamber. This makes the use of LES for combustor flow simulations feasible. In addition, the use of a dynamic procedure to calculate the eddy viscosity, eddy diffusivity and the other parameters occurring due to the filtering of the Navier-Stokes and combustion model equations eliminates the need to specify a priori any constants and to use damping functions near the walls as in RANS or in constant coefficient Smagorinsky models.

As far as the accuracy of the numerical simulations in which turbulent combustion phenomena are of interest is concerned, LES should give better predictions compared to RANS because it is able to more accurately simulate the turbulent mixing phenomena present in these flows. Though the use of a second-order RANS closure instead of the widely popular two-equation linear eddy-viscosity models to model turbulence effects in the strong swirling flow inside the com-

burnstors would probably improve the quality of the predictions of the gas phase dynamics it is still unclear that their use in realistic full combustor geometries will make an important difference compared to linear models. Even though combustion takes place at the smallest scales, capturing the large scales in a flow as complex as the one in the combustion chamber of a realistic combustor geometry is a very difficult task, even for a second-order RANS closure. In fact, recently Pitsch (2000) showed for a much simpler geometry that in terms of predicting the reactive flow, LES is superior to an 'ideal' RANS model, if the same combustion models were used in both calculations. The RANS flowfield was calculated by time averaging the well resolved LES fields. This RANS flowfield is arguably superior to any RANS field produced by a complex RANS closure. Unfortunately, we are not aware of any RANS simulations for realistic combustors that used Reynolds-stress closures.

Complex combustor

This section discusses the cold simulations of the flow in a complex Pratt & Whitney combustor geometry with focus on the validation results. Reference is made to Mahesh et al. (2001) for a detailed discussion of this flow including visualization of the unsteady solution. The computation in the full combustor geometry includes the effects of flow bleed and transpiration. Detailed comparisons of mass-flow splits and pressure drops across the main components of the combustor were made with the available experimental data. The geometry in the symmetry plane $z = 0$ along with contours of the absolute value of the velocity field are shown in Fig. 3. The Reynolds number in the pre-diffuser inlet section defined with the bulk velocity in the inlet section and a characteristic length scale $L = 1''$ is around 500,000 while it assumes a value around 150,000 in the main (core) swirler channel. The computational grid contained around 1.8M control volumes. Typical distances (in wall units) from the center of the first row of cells to the walls ranged from 10 to 100. As we already pointed out, given the physics of interest in this flow, accurate resolution with LES of the attached wall boundary layers is not essential. Turbulent fluctuations from a separate calculation in a periodic pipe sector of identical shape as the pre-diffuser inlet section are fed at the inlet. In the experiment fuel is injected at the tip of the downstream part of the injector. The mass flow rate for the fuel is matched in our simulation. Interestingly, the RANS and LES predictions for the pressure drop across the different components of the combustor are very close (within 6,000 Pa for 5 out of the 6 stations). However, as shown in Table 2, LES does overall a better job to predict the mass flow splits through the swirlers and the inner and outer dilution holes. LES predictions are within 10.5% of the

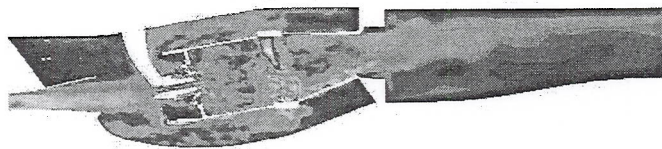


Figure 3. COMPUTATIONAL DOMAIN IN THE $x-y$ SYMMETRY PLANE $z = 0$ WITH CONTOURS OF THE INSTANTANEOUS ABSOLUTE VALUE OF THE VELOCITY FIELD FOR THE FLOW IN THE PRATT & WHITNEY FULL COMBUSTOR GEOMETRY

Location	LES	LES	RANS	RANS
	Error	Error	Error	Error
	%	%	%	%
	Q_{total}		Q_{total}	
OD dil. hole	3.1	0.8	11.4	3.2
ID dil. hole	3.5	0.5	7.5	1.1
Core swirler	10.3	0.14	8.4	0.11
OD swirler	7.5	0.35	13.5	0.63
Guide swirler	0.4	0.02	18.9	0.84

Table 2. COMPARISON OF MASS FLOW SPLITS IN THE PRATT & WHITNEY FULL COMBUSTOR GEOMETRY

experimental measured values for the mass splits through the swirlers, but more importantly within 4% for the total discharges through the swirlers, inner and outer dilution holes. The errors as percentage of the total inlet discharge, shown in the second column of Table 2, are much lower.

Front-end model

Cold flow simulations were performed in the front end Pratt & Whitney test rig geometry. This geometry has the same fuel injector and combustion chamber as the entire combustor, but air is fed to the injector by a cylindrical plenum, the inner and outer diffuser channels are absent and the main combustor chamber does not have dilution holes on the surrounding walls. The interest in simulating the flow in this geometry is the availability of detailed

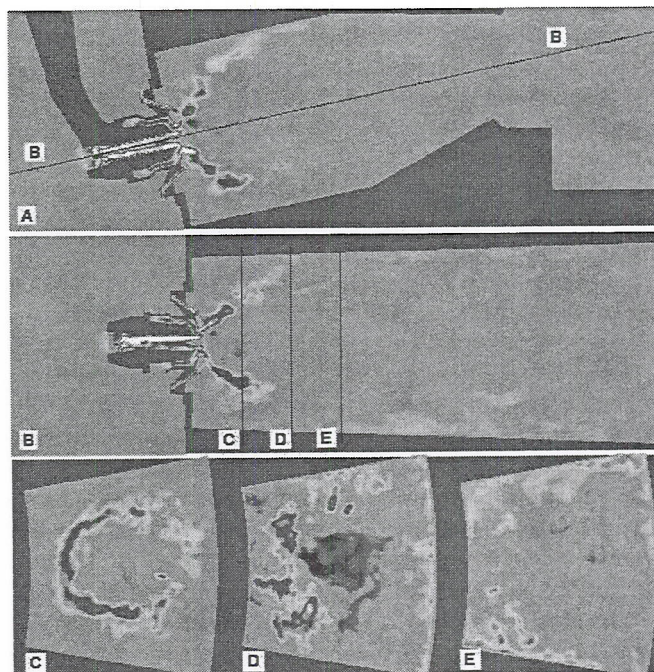


Figure 4. FINE GRID LES SOLUTION FOR THE FRONT END COMBUSTOR GEOMETRY; CONTOURS OF THE INSTANTANEOUS STREAM-WISE VELOCITY COMPONENT (a) IN THE $x-y$ SYMMETRY PLANE ($z=0$), (b) IN A PLANE CONTAINING THE MAIN SWIRLER SYMMETRY AXIS, PERPENDICULAR TO THE $z = 0$ PLANE, AND AT SEVERAL DOWNSTREAM LOCATIONS (c) $x = 1.1''$, (d) $x = 2.2''$, (e) $x = 3.4''$

LDV velocity profile measurements in the main combustion chamber which can be used to fully validate the accuracy of our solver for a geometry of comparable complexity as the full combustor. The Reynolds number in the main swirler channel of the injector is close to 100,000.

The complexity of the geometry and flow inside the test rig is illustrated in Fig. 4 which shows some sections of the computational domain along with contours of the stream-wise velocity in the symmetry plane ($z=0$), in a plane containing the main swirler symmetry axis, perpendicular to the $z = 0$ plane, and at several downstream locations situated respectively at $x = 1.1''$, $x = 2.2''$ and $x = 3.4''$ from the injector for the statistically steady solution obtained on a fine mesh. The main feature observed in these plots is the formation of a relatively large recirculation region downstream of the injector due to the swirling jet coming out from the injector into the main combustor chamber. Prediction of the correct dimensions of the recirculation region along with the variation of the jet width with distance from the injector are two of the main challenges in simulat-

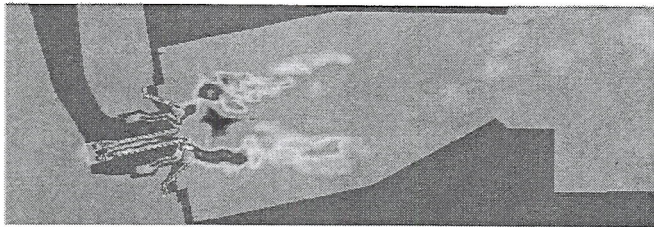


Figure 5. COARSE GRID LES SOLUTION; CONTOURS OF THE INSTANTANEOUS STREAMWISE VELOCITY COMPONENT IN THE $x - y$ SYMMETRY PLANE ($z = 0$)

ing this flow. In particular, RANS simulations of this flow conducted both at Pratt & Whitney using an in-house $\kappa - \epsilon$ code and at Stanford using a commercial software (Fluent) failed to correctly predict these quantities away from the injector, though they were able to fairly successfully predict all the three velocity components immediately downstream of the injector. This is evident from comparison of the RANS profiles with the experimental data symbols in Fig. 6. Interestingly, the Pratt & Whitney RANS simulation was able to accurately capture the pressure drop across the injector (within 2%), while FLUENT yielded a much bigger error ($\sim 20\%$). This is attributed to different grid densities inside the injector. Two grids were generated in the present LES simulations: a coarser grid containing around 2.2M control volumes and a finer containing around 4.5M control volumes. Contours of instantaneous streamwise velocity components are shown in Figs. 5 and 4a for the solutions obtained on the two grids at statistically steady state. Though, for the simulation on the coarser mesh the prediction of the mean pressure drop across the injector (4588 Pa) was found to be very close to the experimental value (4500 Pa), the agreement with the experimental data for the velocity profiles was not found to be much superior to results obtained from RANS simulations. In particular, the spreading of the jet away from the injector was substantially underpredicted. This can be seen by comparing the streamwise velocity profiles at the downstream station $x=2.1''$ from the injector in Fig. 6. The reason for this is that insufficient grid resolution causes the (conical shaped) detached shear layers that are initially shed at the correct angle from the injector (this is expected because all models do a fairly good job in predicting all the velocity components immediately downstream of the injector) to curve toward the injector centerline due to a too high rate of decay of azimuthal momentum inside the initial region of these layers. This results in a much reduced recirculation region compared to the fine grid solution (see Fig. 4) where the detached shear layers are seen to extend up to the lateral

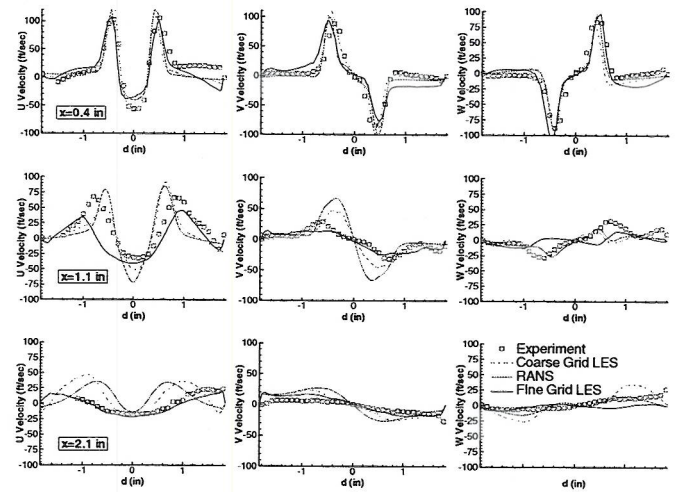


Figure 6. COMPARISON BETWEEN FINE GRID LES, COARSE GRID LES, RANS (FLUENT) AND EXPERIMENT (PRATT & WHITNEY) FOR THE GAS PHASE VELOCITY (STREAMWISE, RADIAL AND SWIRLING) COMPONENTS IN THE PRATT & WHITNEY COMBUSTOR AT THREE STATIONS SITUATED AT $x = 0.4''$, $x = 1.1''$ AND $x = 2.1''$ DOWNSTREAM OF THE INJECTOR

walls of the main combustor chamber. The angle between the injector axis and the conical shape corresponding to the detached layers is approximately constant at 55° . The shedding of vortex tubes due to the Kelvin-Helmholtz instabilities in the detached shear layers is clearly observed. The fine grid solution in Fig. 4 displays the right features corresponding to the flow in the test rig geometry at the specified conditions. This also results in better quantitative predictions for the velocity profiles (see Fig. 6), especially away from the injector where as clearly observed in the mean streamwise velocity profile at $x = 2.1$ from the injector, the level of agreement between the LES fine-grid solution and the experiment is clearly superior to the one observed for the RANS or the LES coarse-grid solutions. However, some differences between the experiment and the fine-grid LES results remain (e.g., compare the streamwise velocity profiles at the $x=1.1''$ station). These differences may occur because the flow is under resolved in some regions. We plan to address this by performing one additional calculation on a very fine mesh (14 millions cells).

The time taken for the cold flow calculation in the full Pratt & Whitney combustor geometry is very reasonable (3,200 CPU hours, or about 100 wall-time hours when the job is run on 32 processors). However, computations in the front-end model are still expensive (110,000 CPU hours) in spite of the implicit algorithm speedup of a factor of six.

This is because the timestep is now limited by accuracy; it is limited by the high flow speeds through the channels of the three swirlers. In normalized terms, the time-step that the calculations are being currently run are the same as that for the simple coaxial combustor. The high cost for the front-end model is therefore the price paid by unsteady simulations in general (including unsteady RANS) and is not peculiar to LES. We are presently investigating the exact requirements of grid resolution and quality inside the injector region such that the time-step could be increased without compromising accuracy.

TWO-PHASE FLOW SIMULATIONS IN THE PRATT & WHITNEY GEOMETRY

Over the last past decade use of LES for studying turbulent combustion phenomena has become more and more common. A good overview of these efforts and of the combustion models used in these simulations is given in Veynante & Poinso (1997). However, there are very few reacting flow simulations in combustor geometries using LES (even in simpler co-axial combustor chambers). Two such simulations were recently reported by Pierce and Moin (2001) who used their own flamelet / progress variable model and by the group in CERFACS, France who are using a Thickened Flame model (Colin et al., 2000) to model combustion in perfectly premixed flames. Recently, they extended their model for simulation of partially premixed flames (Legier et al., 2000). Though considerable understanding of the flow physics and turbulent combustion in gas combustors was achieved from these simulations, the results are not directly applicable to real combustors. For instance, the flow through the injector was not part of these calculations and the overall geometry of the combustion chamber was over simplified compared to that of a real combustor. Thus, there is a real interest from the industry and research community in performing such simulations in full combustor geometries.

Spray breakup simulation in the front-end model

The stochastic model along with the hybrid particle-parcel approach were used to simulate the spray evolution from the Pratt & Whitney injector. The experimental data set was obtained by mounting the injector in a cylindrical plenum through which gas with prescribed mass-flow rate was injected. The gas goes through the main and guide swirler to create a swirling jet into the atmosphere. Liquid film is injected through the filmer surface which forms an annular ring. The liquid mass-flow rate corresponds to certain operating conditions of the gas-turbine engine. Measurements of the droplet distribution and liquid mass flux

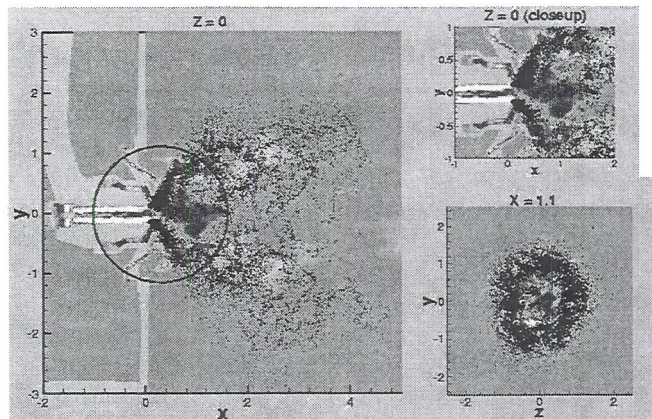


Figure 7. EVOLUTION OF SPRAY FROM A PRATT & WHITNEY INJECTOR: CONTOURS OF AXIAL VELOCITY SUPERIMPOSED WITH PARTICLE SCATTER PLOT

in the radial direction at two different axial locations away from the injector were performed. Gas-phase statistics for mean and rms velocities is also available at these locations. The outside air-entrainment rates were measured and prescribed as inflow conditions. A snapshot of the spray evolution in the $z = 0$ plane along with the gas-phase axial velocity contours is shown in Fig.7. The hybrid-approach used herein gives a dynamical picture with correct spray angle. Around 3.5 million particle trajectories were simulated which represent around 15 million droplets within the combustor. Such an extensive particle-tracking provides very good estimates of the liquid mass-flow rates, the droplet-distributions, and Sauter mean diameters at desired locations. The agreement with the experimental data at different axial locations is within 5% and is considerably improved compared to RANS-type computations. The details of the experimental data and validation results are not shown in this paper for proprietary reasons.

This computation was performed on 96 processors. The domain decomposition is based on the optimal performance of the Eulerian gas-phase solver. Due to breakup, a large number of droplets are created in the vicinity of the injector. With the hybrid approach, the total number of computational particles tracked after 6 ms is around 3.5M, which represents approximately 13M droplets. This includes around 150,000 parcels. The distribution of particles on the 96 processors is shown by the histogram in Fig. 8. This implies that less than 30% of the total number of processors contain more than 10,000 computational particles. A preliminary solution to this problem is to use larger number of processors, which would reduce the maximum number of computational particles per processor. As load

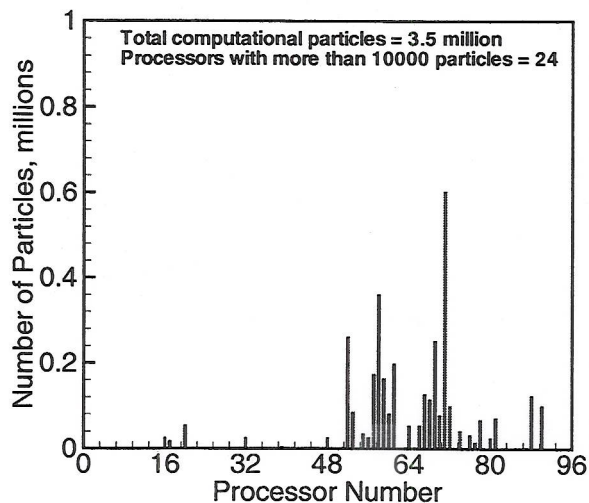


Figure 8. LOAD BALANCE FOR SPRAY BREAKUP SIMULATION

balancing seems to be an important bottleneck for large-scale simulations when spray atomization is present we are investigating several approaches. One better option, we are in the process of implementing, is to develop an alternative domain-decomposition scheme with dynamic load balancing and additional weights for the cells containing particles.

Reacting-flow simulation in the complex combustor

A reacting flow simulation in the same full combustor geometry described in a previous subsection was initiated starting from the gas-phase incompressible solution. We are simulating only the domain corresponding to one injector of the full combustor. A Jet A flamelet library for gas-turbine operating conditions (corresponding to the experimental setup) was generated. The chemical mechanism for the two component surrogate fuel (80% n-Decane and 20% 1,2,4-Tri-methyl-benzene) for Jet A contains approximately 1000 elementary reactions among 100 chemical species. Diversion of the outer diffuser air to secondary systems and transpiration through the liners of the main combustion chamber is specified according to the experimental data.

The Reynolds number in the inlet section of the diffuser is around 600,000. The Reynolds number is defined with the radial height of that section and the mean velocity in the same section. The Reynolds number inside the main swirler channel is about 150,000.

Initially, a calculation without droplets was run. The

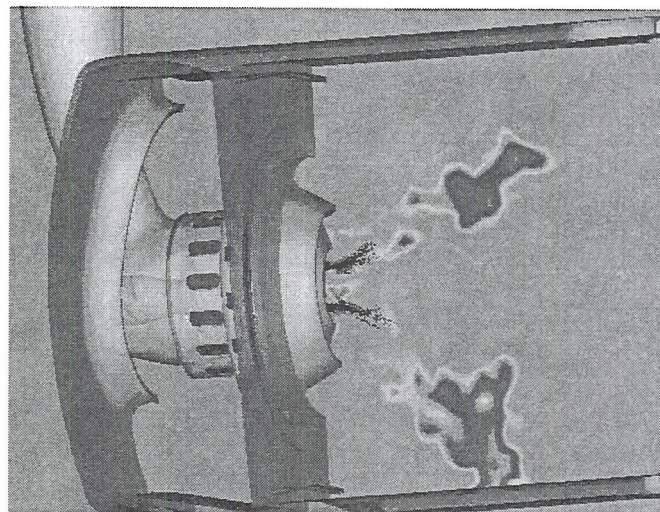


Figure 9. EVAPORATING DROPLETS SUPERIMPOSED ON THE INSTANTANEOUS TEMPERATURE FIELD IN THE REACTING FLOW SIMULATION IN THE PRATT & WHITNEY COMBUSTOR

combustion model is turned on, and we consider that the fuel is evaporating instantaneously in the fuel inlet section. The boundary conditions for the gas phase in the fuel inlet sections were specified such as the mass fuel discharge is equal to the measured value. Once an initial solution (gas phase) without sprays (the flamelet / progress variable combustion model was active in this initial step) was obtained, large liquid fuel droplets are injected in the fuel inlet section to match the measured fuel inlet discharge. Of course, we stop injecting gaseous fuel in the fuel inlet section. Due to the atomization process, the droplets break into smaller particles and eventually evaporate. At this stage of the flow we are tracking only about 100,000 particles, but by the time we will get to statistically steady state for the full coupled (evaporating sprays with combustion) model, we expect this number to be in the order of millions. As described in a previous section we are using a hybrid approach to keep the total number of independent particle trajectories that have to be independently tracked to a reasonable level. A picture of the evaporating sprays superimposed on contours of the instantaneous temperature field is shown in Fig. 9. As the reacting-flow calculation is still in the initial phases, the temperature is higher in the region corresponding to the detached shear layers where the mixture fraction values are relatively high (based on the the non-reactive case with a passive scalar, Z , used to initialize the reacting flow simulation). An initial field for the progress variable was obtained by assuming fast chemistry conditions at the first time step in the reacting flow simulation. At this ini-

tial stage the high temperature region is situated inside the detached shear layers that carry most of the fuel that enters the main combustion chamber. In the regions downstream of the dilution holes the temperature decays rather sharply due to the mixing with the cooler air from the inner and outer dilution channels. We are in the process of running this calculation and evaluating the requirements in terms of grid density needed to perform accurate simulations of the reacting flow in complex combustors of realistic geometry at operating conditions.

SUMMARY AND FUTURE PLANS

In his paper we presented the main features of a three-dimensional, Large eddy simulation two-phase flow code using unstructured meshes to simulate non-reacting and reacting flows through realistic combustor geometries. The solver was parallelized using domain decomposition and the Message Passing Interface (MPI). For validation purposes the results obtained using the present unstructured LES solver were compared with experimental data and computational results from other established LES codes for a wide range of flows ranging from unsteady laminar to fully turbulent. These results were reported in Mahesh et al. (2000, 2001). The present paper provided an overview of the basic numerical schemes and algorithms for the gas phase solver and Lagrangian particle tracking module used in two-phase flow applications, as well as of the combustion and spray models presently implemented into the LES code. The use of these models was tested and demonstrated. In the second part of the paper, results of a series of test cases used to validate the numerical model and the implementation of these models for realistic combustor geometries was presented. Overall, these test cases prove the capacity of the present solver to perform robust and accurate simulations in realistic combustor geometries. Results from several of these simulations show the superior predictive capabilities of LES techniques compared to RANS based solvers for predicting flow, turbulent mixing and combustion phenomena in combustors.

Some of our future plans are summarized below:

- Complete the spray-breakup simulation in the Pratt & Whitney front-end validation geometry. This will serve as the main validation case of the spray atomization models in our code
- Address the issue of load-balancing due to spray and investigate dynamic domain-decomposition techniques for Eulerian-Lagrangian computations of spray.
- Implement a multi-level version of the geometric multi-grid algorithm for the pressure equation solver and investigate the advantages of using multigrid techniques

to accelerate convergence of the momentum and scalar transport equations.

- Implement commutative filters to estimate more accurately the filtered quantities that have to be evaluated in the dynamic procedure and to implement LES models with explicit filtering in which the filter width can be specified a priori by the user instead of being dictated by the local grid spacing.
- Calculate the reacting flow in the full Pratt & Whitney geometry and validate by comparing with the experimental data.
- Start integrating the LES reacting flow solver with an unsteady RANS solver (TFLOW) used to simulate the flow in the compressors, turbines and secondary systems with the goal of producing the first ever fully integrated calculation of a gas turbine engine.

ACKNOWLEDGMENT

We would like to acknowledge the U.S. Department of Energy for its generous financial support under the Accelerated Strategic Computing Initiative (ASCI) program. Computational support was provided by the Department of Energy and the Lawrence Livermore National Laboratory. We are also very grateful to Pratt & Whitney's combustor group for providing detailed experimental data to validate our code and for their constant support and many important contributions to the completion of this work.

REFERENCES

- APTE, S.V., MAHESH, K., & MOIN, P. 2002 LES of particle-laden swirling flow in a coaxial combustor. *to be submitted to Int. J. of Mult. Flows.*
- BIRKBY, P., CANT, T., DAWES, W.N., DEMARQUE, A., DHANASEKARAN, P.C., KELLAR, W., RYCROFF, N.C., SAVILL, A.M., EGGELS, R.L.G. & JENNIONS, I.K. 2000 CFD analysis of a complete industrial lean premixed gas turbine combustor. *ASME Paper 2000-GT-0131.*
- COLIN, O., DUCROS, F., VEYNANTE, D. & POINSOT T. 2000 A thickened flame model for large eddy simulations of turbulent premixed combustion. *Phys. Fluids* 12(7), 1843-1863.
- CROCKER, D.S., NICKOLAUS, D. & SMITH, C. 1998 CFD modeling of a gas turbine combustor from compressor exit to turbine inlet. *ASME Paper 98-GT-0184.*
- ECCLES, N.C. & PRIDDIN, C.H. 1999 Accelerated combustion design using CFD. *XIV ISABE Paper 99-7094.*
- GOROKHOVSKI, M. & APTE, S.V. 2001 Stochastic sub-grid modeling of drop breakup for LES of atomizing spray. *Annual Res. Briefs, Center Turbulence Research, Stanford University*, 169-176.

- KOLMOGOROV, A. N. 1941 On the log-normal distribution of particle sizes during break-up process. *Dokl. Akad. Nauk. SSSR* **31**(2), 99-101.
- LEGIER, P., POINSOT, T. & VEYNANTE, D. 2000 Dynamically thickened flame large eddy simulation model for premixed and non-premixed turbulent combustion. *Proceeding of the Summer Program, Center for Turbulence Research, NASA Ames/Stanford University*, 157-168.
- MAHESH, K., CONSTANTINESCU, G., APTE, S., IACCARINO, G. & MOIN, P. 2001 Large eddy simulation of gas turbine combustors. *Annual Res. Briefs, Center Turbulence Research, Stanford University*, 3-18.
- MAHESH, K., CONSTANTINESCU, G., APTE, S., IACCARINO, G., HAM, F. & MOIN, P. 2002 Progress toward large eddy simulation of turbulent reacting and non-reacting flows in complex geometries. *Annual Res. Briefs, Center Turbulence Research, Stanford University*, 3-25.
- MAHESH, K., CONSTANTINESCU, G. & MOIN, P. 2003a A numerical method for large eddy simulations in complex geometries. invited paper, *Second MIT Conference on Computational Fluid and Solid Mechanics*, Boston, MA.
- MAHESH, K., CONSTANTINESCU, G. & MOIN, P. 2003b A new time-accurate finite volume fractional step algorithm for prediction of turbulent flows on unstructured hybrid meshes. *to be submitted to Journal of Computational Physics*
- MALECKI, R., RHIE, C., MCKINNEY, R.G., OUYANG, H., SYED, S.A., COLKET, M. & MADABHUSHI, R.K. 2001 Application of an advanced CFD-based analysis system to the PW6000 combustor to optimize exit temperature distribution - Part I: Description and validation of the analysis tool. *ASME Paper 2001-GT-0062*.
- O'ROURKE, P. J., & AMSDEN, A. A. 1987 The TAB method for numerical calculations of spray droplet breakup. *SAE Tech. Paper*: 872089.
- PETERS, N. 1984 Laminar diffusion flamelet models in non-premixed turbulent combustion *Prog. Energy Combustion Sciences*, **10**, 319-339.
- PIERCE, C.D. & MOIN, P. 2001 Progress variable approach for large eddy simulation of turbulent combustion. *Report TF - 80*, Flow Physics and Computation Division, Mechanical Engineering Dept., Stanford University, Stanford, California.
- PITSCH, H. 2002 Improved pollutant predictions in Large-Eddy Simulations of turbulent non-premixed combustion by considering scalar dissipation rate fluctuations. *Proceedings of the Combustion Institute*, **29**, in print.
- REITZ, R. D. 1987 Modeling atomization processes in high-pressure vaporizing sprays. *Atom. & Spray* **3**, 309-337.
- SOMMERFELD, M. & QIU, H.H. 1991 Detailed measurements in a swirling particulate two-phase flow by a phase-doppler anemometer. *Int. J. of Heat and Fluid Flow* **12**(1), 20-28.
- VEYNANTE, D. & POINSOT, T. 1997 Reynolds averaged and large eddy simulation modeling for turbulent combustion. *New Tools in Turbulence Modeling, Les Houches School.*, O. Metais and J. Ferziger Editors. Springer, 105-135.
- WALL, C., BOERSMA, B.J. & MOIN, P. 2000 An evaluation of the assumed beta probability density function subgrid-scale model for large eddy simulation of non-premixed, turbulent combustion with heat release. *Phys. of Fluids* **12**(10), 2522-2529.